RESEARCH PAPER

Development and Application of TDR Mini-Probes for Monitoring Moisture in Small-Scale Laboratory Tests

Pengju Qin[1,2] · Yongfeng Deng[5] · Yujun Cui[3] · Weimin Ye[4]

Abstract

The time domain reflectometry (TDR) method has been widely used to explore and track soil moisture. It is necessary to research mini-probes for reducing the influence of the transducer on soil measurement, which encountered many challenges, especially as the transducers are used for studying small-scaled laboratory tests of stiff clay. To overcome these problems, three-wire mini-probes were developed and applied in the present work. Initially, a two-dimensional (2D) weighting theory and numerical simulations were adopted to preliminarily determine the rod spacing (4–4.5 mm) and diameter (0.47–0.63 mm). Subsequently, needle and drill mini-probes were designed to conduct experimental calibration. It was reasonable to employ a 3 cm probe for measurement and a linear equation that related $K_a^{1/2}$ with θ was obtained. Finally, mini-probes were applied to measure water content of compacted and intact stiff clay specimens during continuous desiccation and intact Téguline clay column during wetting, indicating that the mini-probes have the acceptable workability for measuring the moisture of compacted/intact stiff clay undergoing desiccation or wetting processes.

Keywords Stiff clay · Time domain reflectometry · Mini-probe · Sampling area · Dielectric constant · Volumetric water content

1 Introduction

Time domain reflectometry (TDR) technique is applied widely to track soil moisture in the agriculture and engineering practice [1–5]. The TDR probes are often fabricated using stainless steel or brass rods and so forth for feasible penetration into low-density soil [6–8].

Usually, the probe is preset to be longer than 5 cm [7] to monitor the water content of soil in the in situ field and large-scaled mock-up tests in the laboratory. Moreover, it is inevitable to encounter brittle intact soil in the in-suit field and small-scaled specimens in laboratory that are usually adopted to understand hydraulic behavior in geotechnical practice, such as small-scale laboratory infiltration tests and laboratory column experiments on cation diffusion [9, 10]. However, the traditional commercial probes, exhibiting a long length, large diameter and wide spacing, can be hard to be mounted into the measured soil, even damage the soil and influence measurement accuracy. Therefore, it is necessary to develop novel TDR mini-probes to satisfy the experimental and practical requirements.

In addition, it is necessary to know the measurement area of the probe, which preliminarily determines the dimension of the probe according to the size of the specimen. The region of the porous material where TDR probe measures was defined as the sampling volume [11] and it has a significant impact on the response of wave propagation. The voltage distribution around the probe's rods

✉ Yongfeng Deng
noden@seu.edu.cn

1 College of Civil Engineering, Taiyuan University of Technology, Taiyuan 030024, People's Republic of China

2 Shanxi Transportation Technology Research and Development Co. Ltd., Taiyuan 030032, China

3 Ecole des Ponts ParisTech, UR Navier/CERMES, 6-8, av. Blaise Pascal, Cité Descartes, 77455 Marne-la-Vallée, France

4 Department of Geotechnical Engineering, College of Civil Engineering, Tongji University, Shanghai 200092, People's Republic of China

5 School of Transportation, Southeast University, SEU Avenue 2#, Jiangning District, 211189 Nanjing, People's Republic of China

was examined and a balanced transmission contour between the two conductors with polarity (e.g., + 1 V, − 1 V) was found [12]. Based on analytical solutions of probes with two-rods, the energy density (ED) distribution was related to the sampling volume by approximating weighting method that was further validated in the case of multi-rods [13, 14]. A numerical method to solve the Laplace equation for computing the energy density distribution in a two-dimensional (2D) plane was introduced to identify the sampling area around the TDR probe [15]. The numerical approach was also used to calculate the energy density distribution on grounds of various configurations [11, 16, 17]. Based on the spatial weighting analysis of the electromagnetic field using a seepage analysis software, a design of TDR penetrometer was optimized [18]. To derive the sampling volume of the probe, the 2D weighting method was extended to a three-dimensional (3D) description and computed the sampling volume of the probe under several conditions [19]. Therefore, in this work, combining the weighting method and the numerical simulation was adopted to design and optimize mini-probes.

Experimental research was often performed to develop and calibrate TDR probes before the practical engineering applications. A probe made with two paralleled rods with a length of 21 mm was used to measure volumetric water content of clay and sandy clay and found that the measurement was accurate for the soil with a density in the range 1.0–1.5 g/cm³ as the volumetric water content was higher than 0.07 m³/m³ [8]. A short TDR probe with a length of 25 mm was also developed for silica sand measurement with a short TDR pulse rise time of 25 ps [9]. A homemade TDR probe was used to monitor volumetric water content of small stiff clayed specimens in the laboratory [10]. Non-invasive TDR probes were also developed to measure the water retention curve of loess during transient evaporation [5]. Reduction of probe length may result in errors and uncertainties [20, 21], but there is still limited research about the performance of mini-probes, such as the influence of detailed materials and probe application conditions, etc. It was especially difficult to use mini-probes for measuring water content of stiff clay and necessitated to be further investigated for convenient installation and less damage to the measured soil.

This study aimed to develop and calibrate miniature probes for application of the moisture measurement of intact/compacted stiff clay in the laboratory. In detail, based on a 2D weighing theory, numerical simulation was introduced into the present work to determine sampling area and optimize the size parameters of mini-probes. Furthermore, a series of mini-probes, classified into needle and drill probes in terms of rod shape and installation convenience, were calibrated by compacted clay that had different water content. Subsequently, two groups of applications of the mini-probes were performed to demonstrate the validity in the practice, where one is to continuously measure moisture variation of small compacted and intact stiff clayed specimens during drying by installing a probe per specimen, the other is to test a column specimen during wetting by installing four probes to a cylindrical specimen.

2 Theoretical Design of Mini-Probe

The spatial weighting concept and a numerical approach were adopted to compute the sampling area in the plane perpendicular to the TDR rods [11, 13, 15]. A spatial weighting factor ($w(x, y)$) at each plane point for spatial sensitivity was defined [13], which can be expressed as follows in Eq. (1):

$$w(x, y) = |\nabla\Phi(x, y)|^2 / \iint_\Omega |\nabla\Phi_0(x, y)|^2 dA \qquad (1)$$

where $\Phi(x, y)$ is the electrical potential in the heterogeneous field, $\Phi_0(x, y)$ is the electrical potential in the equalized homogeneous field, Ω is the integration domain, and dA is the area of the analysis element. The relationship of $\Phi(x, y)$ and $\Phi_0(x, y)$ can be expressed in the equation $\int K|\nabla\Phi|^2 dA = K_{eq}\int|\nabla\Phi_0|^2 dA$, indicating that the heterogeneous and homogeneous fields with the same boundary condition are equivalent in the aspect of total energies. K is the dielectric constant in a heterogeneous field, K_{eq} is the equalized dielectric constant in the equalized homogeneous field. Application of the spatial weighting function through a numerical approach was extended to predict the spatial distribution of the measurement zone in the plane transverse to the direction of electromagnetic wave propagation. Since the rod's end influence can be ignored [19], the three-dimensional (3D) sampling volume can be simplified into a form of 2D area in the plane transverse to the direction of electromagnetic wave propagation [11]. For a uniform dielectric constant, K_a, the electrostatic potential satisfies the Laplace's equation as follows in Eq. (2):

$$\nabla^2\Phi_0 = 0 \qquad (2)$$

As shown in Fig. 1, the TDR probe comprises with three paralleled metal rods, where the spacing of the outer rods (S), rod diameter (D), and net spacing (s) is defined in the representative plane, perpendicular to the electromagnetic wave propagation. According to the theory proposed in [11], a domain that surrounds the probe and has a given fraction of the total energy in the field can be employed to quantitatively describe the sampling area. In this work, a
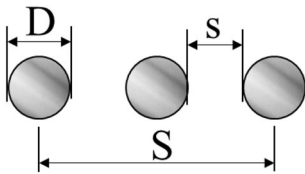
Fig. 1 Representative cross section perpendicular to direction of electromagnetic wave propagation of a three-rod probe

contour of 90% total energy was considered as the sampling area. Subsequently, a 50% sampling area was used to describe probe sensitivity within the area.

Based on the abovementioned theory, the sampling area of the probe depends on the probe's parameters, including the rod's spacing and diameter, which could be simulated by the COMSOL software. According to the relative permittivity scope that stiff clay lies in, an average relative permittivity of 10 was adopted to simulate the porous material during computation, which can be behalf of the material property of the stiff clay. Before computing the sampling area, it is necessary to initially limit a scope of the probe's size. In the light of the energy cylinder distribution area, the probes should be designed with the ratio of the rod diameter to spacing greater than 0.1 were recommended [13], while the ratio that can be as small as 0.02 was suggested in [22]. In this study, the criterion proposed by [22] was used to initially restrict the probe's configuration scope.

In accordance with the initial restriction of the probe's configuration, the theoretical design of the mini-probe was performed. Figure 2 depicts the sampling area percentage (SAP) of the mini-probe with a rod diameter of 0.47 mm and net spacing ranging from 1 to 8 mm. In Fig. 2, only a quarter of the graph for a probe was drawn because of the dual-axis symmetry and eight small graphs for eight mini-probes were patched into two large ones. It is observed that the majority of energy density is concentrated on around the central rod, and the distribution of the energy density is consistent with the previous results obtained in [23]. As the net spacing increases, the sampling area also increases, indicating that the large-scale probe can measure larger areas. In other words, when the net spacing decreases, the sampling area becomes progressively concentrated. Notably, it is better to obtain a relatively uniform energy distribution in the sampling area to reduce the measurement bias generated by the disturbance of the rods to the porous medium in the process of installation [13]. Meanwhile, the narrow rod spacing increases the installation difficulty, which may easily occur as the rods become closer. In contrast, as the rod net spacing increases, the increased sampling area might mislead the measurement of volumetric water content due to the heterogeneity of the material in the localized region. After comprehensively considering the dimensions of soil specimens and installation feasibility, a net spacing of 4 mm or 4.5 mm was preliminarily determined. Furthermore, determination of the diameter of the mini-probe was also conducted. Figure 3 shows quarter photographs of sampling area percentage in a porous material measured by eight types of mini-probes with a diameter ranging from 0.5 to 4 mm. The contour shape is similar to that reported in [11] who derived the sampling area of porous materials. After contrastively analyzing the sampling area percentage of the probe with different diameters, it reveals that the sampling area percentage increases as the rod diameter increases at a given net spacing. Therefore, it is relatively practical to select a probe scheme with a minor diameter to accurately measure a point moisture. Based on the sampling area computation and available materials, a rod diameter ranging from 0.47 to 0.63 mm were determined in this work. Subsequently, the laboratory experiments were performed to calibrate these probes with a net spacing ranging from 4 to 4.5 mm and a diameter ranging from 0.47 to 0.63 mm.

3 Experimental Calibration of Mini-Probe

Although the sizes of the probes can be preliminarily determined by theoretical design, experimental calibration is indispensable to acquire the calibration curves that provide a basis for practical application of the mini-probe. In this section, a Trase BE cable tester was used to capture TDR waveforms of compacted Téguline clay. The calibration curves that relate dielectric constant with volumetric water content are fitted after processing the waveforms.

3.1 Soil Properties

Téguline clay, geologically over-consolidated and classified into the Belgique–London stiff clay group, was extracted in the Albian Paris Basin at Aube, France. The stiff soil is located at depths of 23 m and 43 m below the ground surface and the void ratio varies from 0.327 to 0.347. The specific gravity, liquid limit, and plastic limit are 2.70, 46.9%, and 23.2%, respectively. In accordance with the Unified Soil Classification System, this clay is low to medium plasticity (CL). Besides, the soil is inorganic in nature and the predominant clay mineral comprised of illite (57–65%), chlorite (19–23%), and kaolinite (15–19%). The undisturbed stiff Téguline clay used in the present work was directly extracted from the in-suit field. To maintain the original state underground, the soil after extraction with a diameter of 80 mm and height of 300 mm was sealed in a container that can impose force as same with the original geostress to the specimen and is waterproofed. More
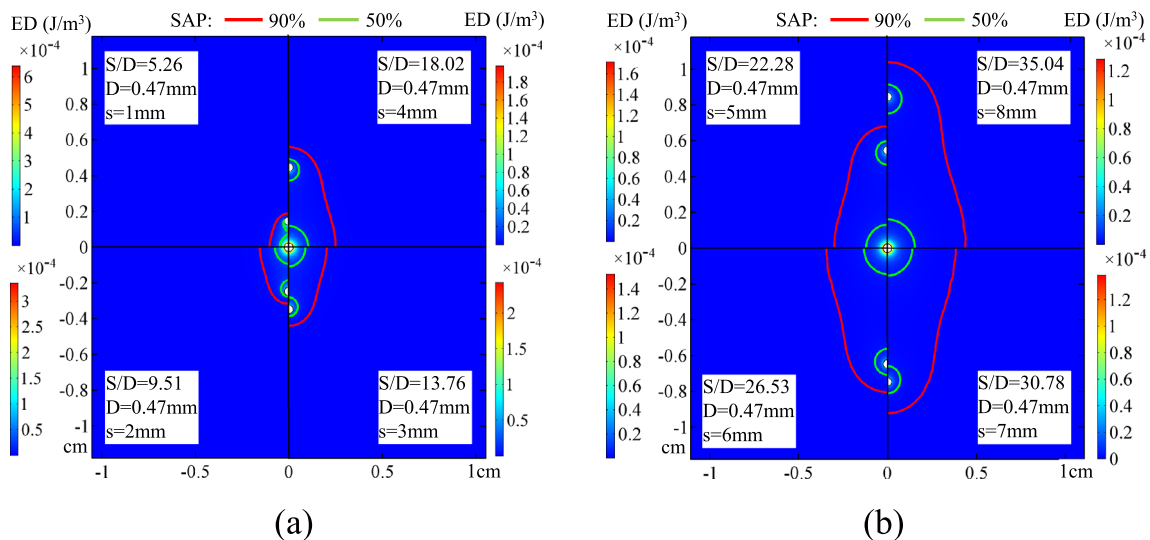
Fig. 2 Quarter photographs of sampling area percentage (SAP) in terms of energy density (ED) of the porous material with an average relative permittivity of 10 for a variety of TDR probes with a rod diameter of 0.47 mm and net spacing s ranging from 1 to 8 mm. **a** Net spacing s of 1–4 mm and **b** Net spacing s of 5–8 mm
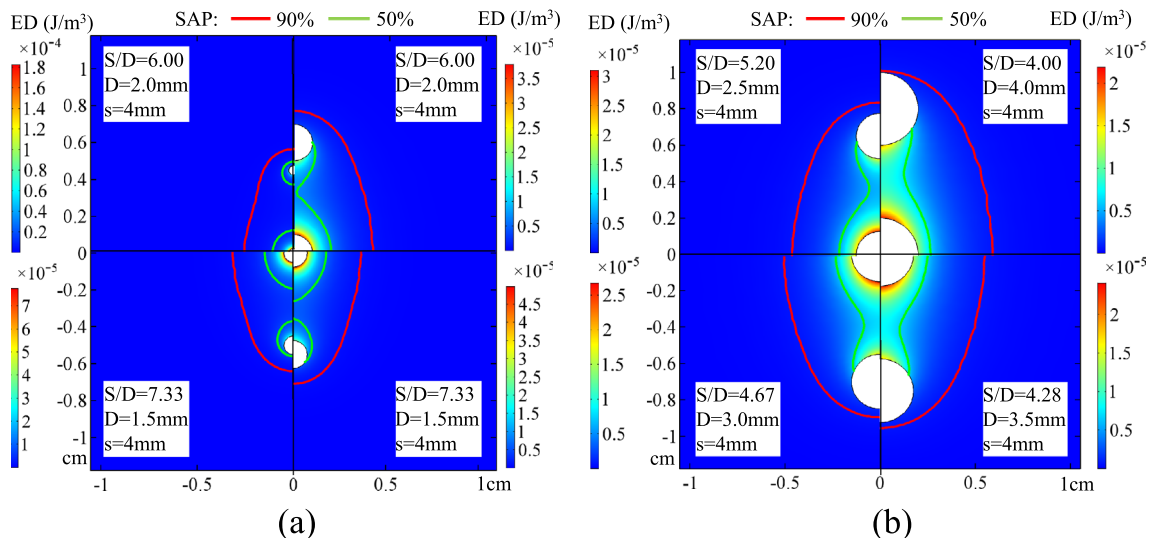

Fig. 3 Quarter photographs of sampling area percentage in terms of energy density of the porous material with an average relative permittivity of 10 for a variety of TDR probes with a net spacing s of 4 mm and rod diameter ranging from 0.5 to 4 mm. **a** Rod diameter of 0.5–2 mm and **b** od diameter of 2.5–4 mm

information about the Téguline clay can refer to the work [24].

3.2 TDR Setup

In Fig. 4, a Trase BE cable tester (Soilmoisture Equipment Corp., Santa Barbara, CA), including a 200-picosecond rise-time instantaneous pulse oscillator, was used to acquire the time domain reflectometry (TDR) waveforms and linked to a computer through an RS232 interface. The

waveforms were recorded using an analysis software package WINTRASE installed in the computer. The coaxial cable combined the tester with the probe. As the cable is too long, it must add additional ohmic resistance and decay the electrical signal [25]. Therefore, the length of the coaxial cable with a conventional 50 Ω resistance in the laboratory is noticeably short, approximately 100 cm, the specimen resistance was assumed to be equal to the total resistance.
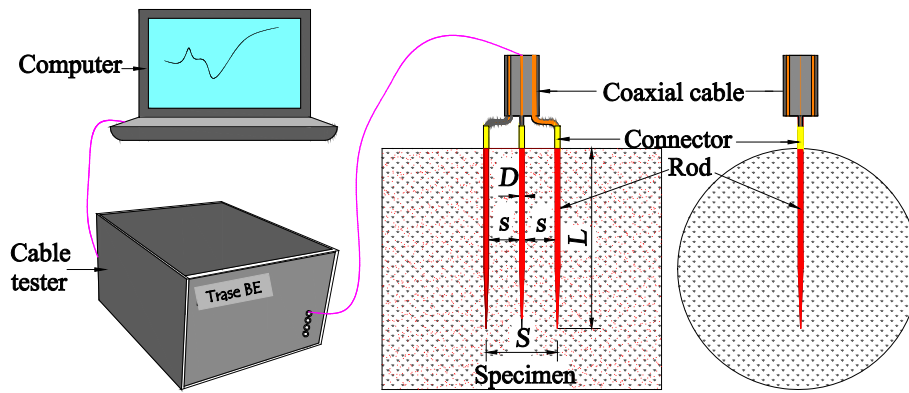
Fig. 4 Schematic sketch of TDR cable tester, TDR min-probe and measured specimen

As mentioned in the theoretical design, two types of three-rod mini-probes were fabricated, where one was a needle-rod probe that can be directly penetrated into the specimen and the other was drill-rod probe that can be drilled into specimen. The miniature needle-rod probe in Fig. 4 was fabricated by the stainless-steel needle with a diameter of 0.63, 0.55, or 0.47 mm and a net rod spacing of 4.5 or 4 mm, as well as the rod lengths that penetrated into the specimens were 26, 28 or 30 mm. Besides, the drill-rod probe comprises three high-speed steel drills with a diameter of 0.5 mm and a net rod spacing of 4 mm and a rod length of 30 mm. All the probes have a length of 11 mm outside the specimen after installation. The dimensional details for the probes are listed in Table 1.

3.3 Calibration Procedure

To develop the probe more suitable for the soil, the dimension, moisture, and dry density of the specimens used for calibration should be similar to the intact state of the soil. The natural stiff Téguline clay has a dry density of approximately 2.0 g/cm^3, and its volumetric water content varies from 10 to 30%, corresponding to a gravimetric

water content of 5–15%. According to the sampling area calculated above, the specimens with a diameter of 50 mm and a height of 40 mm were sufficient to cover the scope of electromagnetic wave transmission.

In the present study, compacted clay was used to calibrate the probes. To prepare the compacted specimens, the clay undergone air dried was crushed into powder and passed through a sieve with a net diameter of 0.4 mm. The powder was sprayed with distilled water until the given water content reached. After sealing for at least 24 h in a box for water homogeneity, the soil was statically compacted into a cylinder with a diameter of 50 mm and height of 40 mm by a stainless-steel mould and piston through controlling the displacement of the piston, the compression of the soil finished until the dry density of the specimen arrived to 2.0 g/cm^3.

After preparation of compacted specimens with different constant water content in terms of the method mentioned above, one set of calibrations was conducted with the needle-rod probes, the other set of calibrations was performed with the drill probes. Prior to probe installation, a plastic guiding cube with three holes, used to ensure that the rods were parallel and equidistant, was fixed to the

Table 1 Mini-probe configuration for calibration and application

Test no.	Rod type	Diameter (mm)	Net spacing (mm)	Probe length (mm)	Outside length (mm)	Calibrated type	Application num	Application type
N1	Needle	0.63	4.5	30	11	Compacted		
N2		0.55	4.5	30			A1	Compacted
N3		0.47	4	30			A2	Intact
N4		0.47	4	28				
N5		0.47	4	26				
D1	Drill	0.5	4	30			A3	Compacted

Note 'N1' represents that probe is made from needle and '1' represents the number of this group of calibration test, while 'D1' represents that probe is made from drill and '1' has the same definition

surface of the cylindrical specimens. The rods were then separately inserted (or drilled) into the specimens one by one until all the three rods were installed with a designated length, as observed in Fig. 4. After the rods were installed into the specimen, the plastic guiding cube was removed. Consequently, a coaxial cable was connected and immobilized to the rods' ends using a homemade shrinkable plastic connector (SP) for TDR measurements, as depicted in Fig. 4. Subsequently, the waveforms were obtained with the WINTRASE. Specifically note that a plastic membrane was used to cover the specimens to avoid water evaporation from the specimens during measurements. The calibration tests were performed under a constant temperature of 20 ± 1 °C.

After acquiring the waveforms, the specimens were oven dried at 105 °C until no further mass change occurred. The water mass change was measured with a precision balance, while the dry density was computed by measuring the size and weight of the specimen. The measured volumetric water content can be calculated by the three-phase concept of soil mechanics. Table 1 lists all the experimental configurations of the six groups of mini-probes.

3.4 Parameters Calculation

The calculation of volumetric moisture content from the dielectric constant is based on the fact that the dielectric constant K_a strongly depends on the water volume within the soil, i.e. the static dielectric constants of pure water and dry soil is equal to approximately 80 and 2, respectively [26]. Additionally, the velocity of electromagnetic wave propagation depends on the dielectric constant of the porous material, which can be expressed as shown below:

$$K_a = (ct_p/2L)^2 \tag{3}$$

where K_a is the dielectric constant of the porous medium, c is the velocity of light (3×10^8 m/s), t_p (s) is the time taken for wave propagation along the rod measured by a TDR meter, and L (m) is the length of the rod inserted into the porous medium.

If the dielectric loss caused by molecular relaxation and electrical conductivity is negligible, the value of the dielectric constant measured by the TDR probe represents the real part of the complex dielectric permittivity [23]. The waveform automatically tracked by the cable tester was recorded by WINTRASE (Soilmoisture Equipment Corp., Santa Barbara, CA). The waveform analysis was performed by a ''dual-tangent'' approach referring to the works in [27] and [28].

Additionally, the volumetric water content θ can also be calculated from the water mass loss measurement as follows:
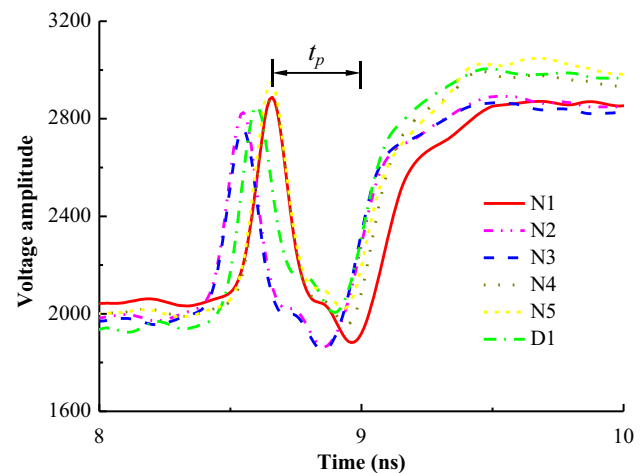

Fig. 5 Waveforms measured by probe N1, N2, N3 and D1 with a penetrated length of 30 mm, N4 is 28 mm and N5 is 26 mm for specimens with volumetric water content of about 24%

$$\theta = \omega \rho_d / \rho_w \tag{4}$$

where ω is mass water content, ρ_d (kg/m^3) is the dry density, and ρ_w (kg/m^3) is the density of water at 4 °C (equal to 1000 kg/m^3).

3.5 Calibration Equation

After acquiring the waveforms, the time (t_p) of wave propagation along the rod can be obtained as plotted in Fig. 5, and the dielectric constant can be calculated by Eq. (3). Moreover, the volumetric water content can also be computed by Eq. (4). The calibration relationship can be discussed by taking into account the influence of the installation pattern, rod diameter, spacing, and length for confirming the feasibility of these mini-probes.

Figure 5 depicts the waveforms measured by different probes for specimens with a volumetric water content of about 24%. To distinctly observe the waveforms acquired as signal travelled in the probe, the time of from 8 to 10 ns is extracted. It can be observed that the waveforms measured by the probes are almost similar in the aspect of shape. As the pulse signal travels to the beginning of the probe, the voltage amplitude quickly increases, followed by a rapid decrease because the signal travels to the part of the probe immersed in the specimen. Therefore, the first peak can be used to determine the starting time of wave propagation along the rods. When the wave is reflected at the end of the rod, the voltage amplitude quickly increases again. It also suggests that not all of the first reflection peak of reflected waveforms are coincident at the same time because of the connection deviation between coaxial cable and rods and fluctuation of signal voltage amplitude. In addition, the waveform between the starting end and the

terminal end of the rods is a little fluctuant rather than straight, which can be attributed to the short wavelength of the electromagnetic wave and short travel trip in the probe. According to the reference [29], the time of pulse arrival at the end of the transmission line is often determined from the intersection of the tangent at the time of the maximum gradient of the second reflection and the tangent at the local minimum amplitude. Since, in this work the local minimum amplitude is absent for the measured soil with a low dielectric constant, the "dual-tangent" approach is used to determine the end time of wave propagation along the rod, which locates around the bending point of the waveform.

Figure 6 depicts the mapping distribution of the measured K_a and θ plane. It observes that the data obtained by probe N2 and N3 fall within a narrow band. The probes of N2 and N3 used in the tests have different rod diameters and spacing, thereby indicating that the rod diameter and spacing have an insignificant influence on the measurement. In addition, a slight difference in the K_a value between N2 and D1 test was observed at a given θ as comparing the mapping distribution of K_a and θ of the compacted stiff clay obtained by needle-rod probe with that by drill-rod probe, suggesting that the installation pattern of the mini-probe has less influence on the calibration relation. This result also confirms that there is no significant difference to measure the water content with probes installed with or without pilot holes [30]. Notably, the mapping relationship between K_a and θ can be relatively concentrated except N4 and N5, indicating that the probe length is a key parameter in the design of mini-probes. This is because as the probe becomes very short, the input and reflected pulses seriously interfere with each other so that it was difficult to correctly determine the point corresponding
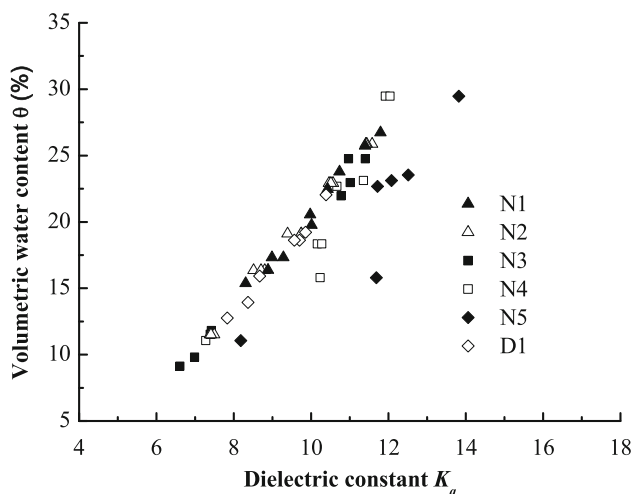
to the end of the probe in the waveform. To improve the accuracy of the mini-probes, the N4 and N5 probes were not used in subsequent investigations.

For further application of these mini-probes, a calibration equation of the measured relationship between K_a and θ should be established. Based on the previous investigations on the calibration method, in which the functions of $K_a^{1/2}$ and was extensively emphasized [31–34], Eq. (5) was thus adopted in this study, which can be expressed as follows:

$$\theta = aK_a^{1/2} + b \tag{5}$$

where, a and b are fitting parameters.

After re-visiting the data in Fig. 6 (except N4/N5), the calibrated equation was fitted as Eq. (6), which can be expressed as follows:

$$\theta = 0.21K_a^{1/2} - 0.46 \tag{6}$$

Note that in this calibration equation, the correlation coefficient R^2 is 0.98, which suggests the feasibility of the proposed mini-probes and the reliability of the fitting parameters. Hence, the values of a and b were 0.21 and − 0.46 for subsequent applications, respectively. Besides, the Root Mean Square Error (RMSE) of volumetric water content obtained by the probe N1, N2, N3 and D1 is 0.66%, 0.66%, 0.78% and 0.54%, respectively. This suggests that the measured results by the probe D1 are closer to those computed by the calibrated equation, while the measured results by the probe N3 is a little more deviated from those computed by the calibrated equation compared with those by another probes.

4 Applications of Mini-Probes

After theoretical design and experimental calibration of the mini-probes, the probes are often used to measure moisture of soil in the process of continuous desiccation and wetting for observing the moisture variation of the soil. In this section, the mini-probes are applied to monitor the moisture variation of the Téguline clay during desiccation or wetting.

4.1 Moisture Measurement During Continuous Desiccation of Specimens

The mini-probes are used to be prepared to track the moisture variation of compacted and intact specimens in the process of desiccation. The compacted specimen with an initial mass water content of 16% was prepared by the same method as mentioned above. The configuration of mini-probes used for measuring moisture of specimens are listed in Table 1. To desiccate the compacted specimen, a

Fig. 6 Mapping distribution of dielectric constant versus volumetric water content

plastic membrane was removed to air desiccate the specimen. After desiccation, the dielectric constant, dimension and water mass loss were recorded. After measurement, the compacted specimen was packed by the plastic membrane and resealed at a chamber to equilibrate moisture distribution in the specimen for 12 h. Subsequently, the procedure was repeated until the water mass content reduced to approximately 4%. Finally, the specimen was oven dried at 105 °C until no further water loss was measured. In accordance with the mass loss and dimension change of the specimen, the measured volumetric water content was obtained. In the light of the dielectric constant and Eq. (6), the calculated volumetric water content was obtained.

In the case of the intact clay specimen, the undisturbed clay was trimmed from the cylindrical core by a saw and then immediately packaged with a plastic membrane to prevent water evaporation. The desiccation and measurement procedure of the intact clay specimen is consistent with that of the compacted specimen. The comparison between the measured and calculated volumetric water content is depicted in Fig. 7. It indicates that the measured and calculated volumetric water content have a maximum error within ± 3% for not only the needle and drill methods, but also the compacted and intact specimens. This application can validate the precision of the mini-probes that can satisfy the requirement of laboratory experiments.

4.2 Moisture Measurement During Continuous Wetting of Intact Téguline Clay Column

Apart from the drying process of soil, the wetting of soil is also common and significant, which can be used to deeply understand the complex infiltration behavior of unsaturated
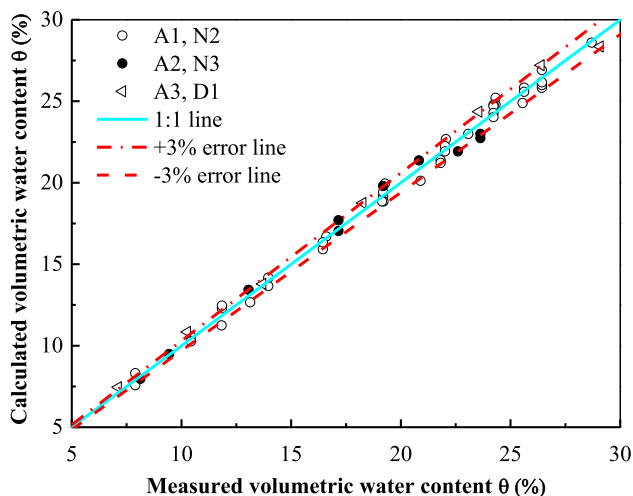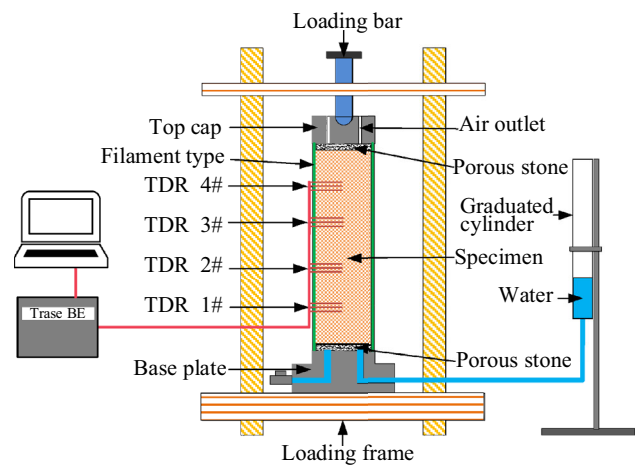

Fig. 8 Schematic graph of Setup for monitoring moisture variation of unsaturated intact Téguline clay

geomaterials. Téguline clay is a potential formation material as nuclear waste disposal in France. During constructing disposal facilities, the clay unavoidably encounters drying and wetting due to ventilation and underground water immersion. Thus, a setup was developed to measure moisture change of intact Téguline clay column in an infiltration test to clarify the water migration process and explore barrier performance of the soil.

The setup, as depicted in Fig. 8, consists of a loading frame, a top cap, a base plate, two porous stones, four TDR sensors and filament type. A loading bar at the top of the loading frame can impose force to fix the intact Téguline clay column. The top cap and the base plate sandwiched the porous stones and the specimen. The base plate has water inlets for water immersing the bottom end of the column out whose air will be exhausted through the air
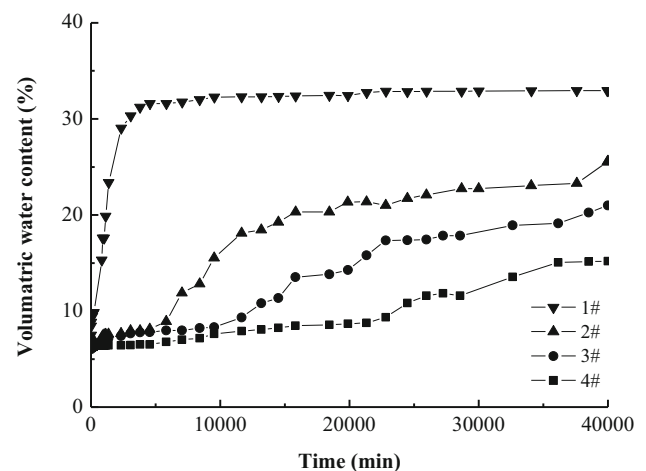

Fig. 7 Comparison between measured and calculated volumetric water content of specimens during continuous desiccation

Fig. 9 Evolution of volumetric water content at different location of the intact Téguline clay with time

outlet in the top cap. Two pieces of filter paper undrawn in Fig. 8 were sandwiched by the porous stones and the specimen that was wrapped by filament type. Moreover, four TDR mini-probes developed in this work were used to trace the moisture change of the corresponding point and the probes were mounted within a drilling frame.

The evolution of volumetric water content at different location of the intact Téguline clay column with time is presented in Fig. 9. It observes that the volumetric water content measured by the TDR sensor 1# rapidly increases in a short time and tends to a slow grow as time sequentially elapses because the 1# mini-probe is closest to the immersion water end that inclines to be saturated. Correspondingly, the closer to the immersion water end, the higher volumetric water content is measured at a given time, which indicates that the initial unsaturated column specimen is adsorbing water. The flowing water volume at every measured point can be computed in terms of the volumetric water content as plotted in Fig. 9, which can further determine hydraulic conductivity as its suction is also measured.

5 Conclusions

To satisfy the demand for measuring water content of small-scaled stiff clay, TDR mini-probes were designed by theoretical optimization, experimental calibration and application validation for determining the practicality of the mini-probes for stiff clay. The main conclusions in this study can be summarized as follows:

1. The 2D weighting theory combined with numerical simulation of electromagnetic wave propagation is an effective method to preliminarily screen the dimension of the mini-probes. Based on this method, it reasonably determined the net spacings of 4.0 mm and 4.5 mm and rod diameters ranging from 0.47 to 0.63 mm of the mini-probes.

2. Upon experimental calibration of the mini-probes, it found that the mini-probe length of 3 cm is reasonable in terms of concentration degree of mapping relationship between the dielectric constant and volumetric water content. Based on the data of the 3 cm mini-probes, a calibration equation that relates $K_a^{1/2}$ with θ was fitted for further application of the probes. Besides, it also found that diameter, spacing and installation pattern had an insignificant influence on the relationship between the dielectric constant and volumetric water content.

3. When the mini-probes are applied to measure moisture variation of compacted and intact Téguline clay specimens undergoing continuous desiccation, the error between measured and calculated volumetric water content is within a scope of ± 3%. For wetting of intact Téguline clay column, the probe nearest water has an obvious increase of the volumetric water content and the values measured by the rest of probes slowly changes, which conforms to the evolution rules as the column specimen adsorbs water. All of these results of the application tests verify the feasibility of the mini-probes.

4. This investigation proposes a method or procedure to develop a TDR probe for specific application in water content measurement. Further attempts would be conducted to optimize this procedure.

Declarations

Conflict of interest On behalf of all authors, the corresponding author states that there is no conflict of interest.

References

1. He HL, Aogu KL, Li M, Xu JH, Sheng WY, Jones SB, González-Teruel JD, Robinson DA, Horton R, Bristow K, Dyck M, Filipović V, Noborio K, Wu QB, Jin HJ, Feng H, Si BC, Lv JL (2021) A review of time domain reflectometry (TDR) applications in porous media. Adv Agron 168:83–155. https://doi.org/10.1016/bs.agron.2021.02.003

2. Miyata S, Mizugaki S, Naito S, Fujita M (2020) Application of time domain reflectometry to high suspended sediment concentration measurements: laboratory validation and preliminary field observations in a steep mountain stream. J Hydrol 585:124747. https://doi.org/10.1016/j.jhydrol.2020.124747

3. Woodall CW, Evans DM, Fraver S, Green MB, Lutz DA, D'Amato AW (2020) Real-time monitoring of dead wood moisture in forests: lessons learned from an intensive case study. Can J For Res 50:1244–1252. https://doi.org/10.1139/cjfr-2020-0110

4. Yang J, Chen HS, Nie YP, Wang KL (2019) Dynamic variations in profile soil water on karst hillslopes in Southwest China. CATENA 172:655–663. https://doi.org/10.1016/j.catena.2018.09.032

5. Mu QY, Zhan LT, Lin CP, Chen YM (2020) Non-invasive time domain reflectometry probe for transient measurement of water retention curves in structured soils. Eng Geol 264:105335. https://doi.org/10.1016/j.enggeo.2019.105335

6. Heimovaara TJ (1993) Design of triple-wire time domain reflectometry probes in practice and theory. Soil Sci Soc Am J 57:1410–1417. https://doi.org/10.2136/sssaj1993.03615995005700060003x

7. Persson M, Haridy S (2003) Estimating water content from electrical conductivity measurements with short time-domain

reflectometry probes. Soil Sci Soc Am J 67:478–482. https://doi.org/10.2136/sssaj2003.4780

8. Amato M, Ritchie JT (1995) Small spatial scale soil water content measurement with time-domain reflectometry. Soil Sci Soc Am J 59:325–329. https://doi.org/10.2136/sssaj1995.03615995005900020008x

9. Kelly SF, Selker JS, Green JL (1995) Using short soil moisture probes with high-bandwidth time domain reflectometry measurements. Soil Sci Soc Am J 59:97–102. https://doi.org/10.2136/sssaj1995.03615995005900010015x

10. Su W, Cui YJ, Qin PJ, Zhang F, Ye WM, Conil N (2018) Application of instantaneous profile method to determine the hydraulic conductivity of unsaturated natural stiff clay. Eng Geol 243:111–117. https://doi.org/10.1016/j.enggeo.2018.06.012

11. Ferré PA, Knight JH, Rudolph DL, Kachanoski RG (1998) The sample areas of conventional and alternative time domain reflectometry probes. Water Resour Res 34:2971–2979. https://doi.org/10.1029/98WR02093

12. Zegelin SJ, White I, Kenkins DJ (1989) Improved field probes for soil water content and electrical conductivity measurement using time domain reflectometry. Water Resour Res 25:2367–2376. https://doi.org/10.1029/WR025i011p02367

13. Knight JH (1992) Sensitivity of time domain reflectometry measurements to lateral variations in soil water content. Water Resour Res 28:2345–2352. https://doi.org/10.1029/92WR00747

14. Knight JH, White I, Zegelin SJ (1994) Sampling volume of TDR probes used for water content monitoring. In: Proceedings of the symposium and workshop on time domain reflectometry in environmental, infrastructure and mining application, Minnesota, USA, September

15. Knight JH, Ferre PA, Rudolph DL, Kachanoski RG (1997) A numerical analysis of the effects of coatings and gaps upon relative dielectric permittivity measurement with time domain reflectometry. Water Resour Res 33:1455–1460. https://doi.org/10.1029/97WR00435

16. Ferré PA, Knight JH, Rudolph DL, Kachanoski RG (2000) A numerically based analysis of the sensitivity of conventional and alternative time domain reflectometry probes. Water Resour Res 36:2461–2468. https://doi.org/10.1029/2000WR900119

17. Robinson DA, Friedman SP (2000) Parallel plates compared to conventional rods as TDR waveguides for sensing soil moisture. Subsurf Sens Technol Appl 1:497–511. https://doi.org/10.1023/A:1026523917731

18. Zhan TLT, Mu QY, Chen YM, Ke H (2015) Evaluation of measurement sensitivity and design improvement for time domain reflectometry penetrometers. Water Resour Res 51:2994–3006. https://doi.org/10.1002/2014WR016341

19. Qin PJ, Liu ZR, Lai XL, Wang YB, Song ZW, Miao CX (2020) A new method to determine the spatial sensitivity of time domain reflectometry probes based on three-dimensional weighting theory. Water 12(2):545. https://doi.org/10.3390/w12020545

20. Stein J, Kane DL (1985) Reply of monitoring the unfrozen water content of soil and snow using time domain reflectometry. Water Resour Res 21:1057–1058. https://doi.org/10.1029/WR021i007p01061

21. Reeves TL, Elgezawi SM (1992) Time domain reflectometry for measuring volumetric water content in processed oil shale waste. Water Resour Res 28:769–776. https://doi.org/10.1029/91WR02895

22. Petersen LW, Thomsen A, Moldrup P, Jacobsen OH, Rolston DE (1995) High-resolution time domain reflectometry: sensitivity dependency on probe-design. Soil Sci 159:149–154. https://doi.org/10.1097/00010694-199515930-00001

23. Robinson DA, Jones SB, Wraith JM, Or D, Friedman SP (2003) A review of advances in dielectric and electrical conductivity measurement in soils using time domain reflectometry. Vadose Zone J 2:444–475. https://doi.org/10.2113/2.4.444

24. Zeng LL, Cui YJ, Conil N, Zghondi J, Armand G, Talandier J (2017) Experimental study on swelling behaviour and microstructure changes of natural stiff Téguline clays upon wetting. Can Geotech J 54(5):700–709. https://doi.org/10.1139/cgj-2016-0250

25. Heimovaara TJ, Focke AG, Bouten W, Verstraten JM (1995) Assessing temporal variations in soil water composition with time domain reflectometry. Soil Sci Soc Am J 59:689–698. https://doi.org/10.2136/sssaj1995.03615995005900030009x

26. Chen RP, Chen YM, Chen W, Chen Y (2012) Time domain reflectometry for water content measurement of municipal solid waste. Environ Eng Sci 29(6):486–493. https://doi.org/10.1089/ees.2010.0489

27. Heimovaara TJ (1994) Frequency domain analysis of time domain reflectometry waveforms. 1. Measurement of the complex dielectric permittivity of soils. Water Resour Res 30:189–199. https://doi.org/10.1029/93WR02948

28. Wraith JM, Or D (1999) Temperature effects on soil bulk dielectric permittivity measured by time domain reflectometry: experimental evidence and hypothesis development. Water Resour Res 35:361–369. https://doi.org/10.1029/1999WR900095

29. Schwartz RC, Casanova JJ, Bell JM, Evett SR (2014) A reevaluation of time domain reflectometry propagation time determination in soils. Vadose Zone J 13(1):1–13. https://doi.org/10.2136/vzj2013.07.0135

30. Topp GC, Davis JL, Annan AP (1982) Electromagnetic determination of soil water content using TDR: II. Evaluation of installation and configuration of parallel transmission lines. Soil Sci Soc Am J 46:678–684. https://doi.org/10.2136/sssaj1982.03615995004600040003x

31. Ferré PA, Rudolph DL, Kachanoski RG (1996) Spatial averaging of water content by time domain reflectometry: implications for twin rod probes with and without dielectric coatings. Water Resour Res 32:271–279. https://doi.org/10.1029/95WR02576

32. Hook WR, Livingston NJ (1995) Errors in converting time domain reflectometry measurements of propagation velocity to estimates of soil water content. Soil Sci Soc Am J 60:35–41. https://doi.org/10.2136/sssaj1996.03615995006000010008x

33. Ledieu J, Ridder PD, Clerck PD, Dautrebande S (1986) A method of measuring soil moisture by time domain reflectometry. J Hydrol 88:319–328. https://doi.org/10.1016/0022-1694(86)90097-1

34. Masbruch K, Ferré TPA (2003) A time domain transmission method for determining the dependence of the dielectric permittivity on volumetric water content: an application to municipal landfills. Vadose Zone J 2:186–192. https://doi.org/10.2113/2.2.186